

A LOW COST CASCADED H-BRIDGE MULTILEVEL CONVERTER WITH DC SIDE SENSOR LESS PHOTOVOLTAIC SYSTEM

¹T.BALARAMAKRISHNA

M.Tech (PID)
JNTU,ANANTAPUR
Andhra Pradesh, India.

²B.THEJASVI

Lecturer
JNTU,ANANTAPUR,
Andhra Pradesh, India

Abstract- Photovoltaic energy conversion becomes main focus of the many researches because of its promising potential as source for future electricity and has many benefits than the other energy sources like wind, solar, ocean, biomass, geothermal etc. In this paper a cascaded H-Bridge (CHB) multilevel converter primarily based photovoltaic (PV) system with no voltage or current sensors at the dc-side is planned using incremental conductance base maximum power point tracking scheme. Eliminating the dc-side sensors simplifies the hardware, resulting in lower price and better reliable-ness of the PV system. A novel scheme estimating the capacitors' voltages from the output ac voltage of the inverter is developed. The scheme permits replacement all dc-side voltage sensors by one voltage sensor at the ac-side of the converter. Moreover, the dc current sensors, conventionally needed for the maximum power tracking (MPPT), also are eliminated. Instead, the outputs from the capacitors' voltage control systems are used for the MPPT. The effectiveness of the projected dc-side sensorless system is simulated on a 2 KW single-phase 7-level CHB converter based PV system. The simulation was done by using MATLAB/Simulink software.

Index Terms— Capacitor-voltage estimation, cascaded H-bridge (CHB) converter, photovoltaic (PV) system, Fuzzy logic controller, MATLAB.

I. INTRODUCTION

In the recent years, the demand for clean and green energy needs top quality output power with low switching losses. It's additionally seen that the soft switching technology develop showing that the demand any will increase by rising efficiency. This trend is predicted to continue in coming years as a result of the energy produced by renewable sources is predicted to satisfy 200th and 500th of the entire wants in 2020 and 2050 respectively. It's additionally witnessed that among these renewable energy sources, solar photovoltaic energy is found to be a promising energy. an important consequence of this case may be a modification of the electric power system from this one, consisting of a comparatively low range of very high power ac generators, to a distributed one, characterized by a very large number of tiny and medium power dc and ac generators provided by renewable energy sources connected to the grid through electronic power converters, the latter adapting the created energy to grid specifications.

In this paper, implementation of multilevel inverter using MPPT based Perturb and Observe algorithm for PV cell is demonstrated. The Output of the system isn't continuous as a result of the variation within the irradiance of solar energy due to the variable output voltage that leads to battery failure. so as to protect

the battery from harm, a DC-DC Buck converter with MPPT primarily based P&O technique is connected in between solar module and battery. By using perturb and observe technique the switch conduction will be controlled which provides the constant voltage to the battery so it will be protected.

Cascaded H-Bridge (CHB) multilevel PV inverters are composed of many "smaller" (in terms of the rated power) full-bridge DC-AC converters (hereafter referred as cells), every of them created by downsized switching devices, that are so less affected by dynamic and static power losses. moreover, because of ability of multilevel topologies to provide the "stepped" output voltages, CHB inverters reproduce sinusoidal waveforms higher than conventional full-bridge inverters with less filter efforts, the entire harmonic distortion (THD) being a perform of the amount of discrete voltage levels exploited to synthesize the output wave. Moreover, the modular structure of CHB inverters is of course well-suited for distributed power conversion, as a result of every cell will be powered by a small PV generator and performs a dedicated MPPT.

Despite of the aforesaid advantages, in CHB inverters, the control of electronic devices switching operation is far a lot of demanding compared to conventional inverters. Moreover, the increased range of switching devices needs a correct analysis of power consumption throughout turn-on and turn-off transients that affects the conversion efficiency. In a very recent paper, a single-phase CHB multilevel PV inverter appropriate for high granularity maximum power point tracking (up to single panel level) was presented. The innovative control strategy adopted in this allowed just one elemental converter to figure in switching mode whereas the others were unbroken either "ON" or "OFF".

The proposed three-phase CHB adopts a mixed staircase-pulse-width modulation (PWM) strategy that drives only 1 power cell at time to work in PWM, while all other cells offer a constant output voltage. Output voltages achieved by every cell may be independently adjusted in order that the maximum power point (MPP) of every PV scheme (connected to the corresponding cell of the inverter) may be on an individual basis tracked. The quantity of sections will coincide with the quantity of solar panels forming the PV system; so, single panel MPPs may be individually adjusted, and also the projected approach may be effectively adopted for single panel distributed conversion schemes. in this project we are implementing the cascaded H-Bridge inverter along individual DC supply and to cut back the Dc supply the Cascaded H-Bridge are linked in parallel also to increases the output voltage level the low frequency transformer is utilized along with every Cascaded H Bridge inverter.

II. CONFIGURATION OF DC-SIDE SENSORLESS CHB-MC BASED PV SYSTEM

Since the output voltage of the PV modules will vary in a very wide range owing to partial shading, the PV modules are historically connected to a set dc-link voltage of the inverter via a dc-dc converter.

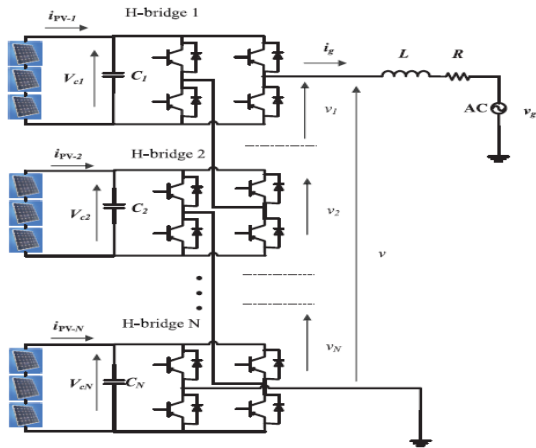


Fig. 1. CHB-MC PV system

However, by introducing the dc-dc converter, the overall efficiency of this configuration is reduced by 4%–10% and also the value and complexness of the system is increased. However, since the CHB-MC permits dominant the individual capacitors' voltages severally, the PV modules may be connected directly to the dc-links, so eliminating need for the dc-dc converters, as shown in Fig. 1.

Conventional control systems for this configuration need N H-bridges, N voltage sensors, and N current sensors at the dc-side. In this paper, a dc-side sensor-less system for the configuration in Fig. 1 is proposed. The main advantage of the projected system, as compared to the traditional ones, is that all dc-side current and voltage sensors are eliminated, that considerably reduces the system's complexness and value. In the projected system, only one voltage sensor is needed to measure the voltage at the ac-side of the CHB-MC. Additionally, one voltage sensor is needed to measure the grid voltage and one current sensor is needed to measure the grid current.

III. PV CONTROL ALGORITHMS & MODULES

Block diagram of the proposed control system is shown in Fig. 2. The ac output voltage v measured at the ac-side of the CHB-MC is used to estimate the capacitors' voltages in the capacitors' voltages' estimation module (CVEM).

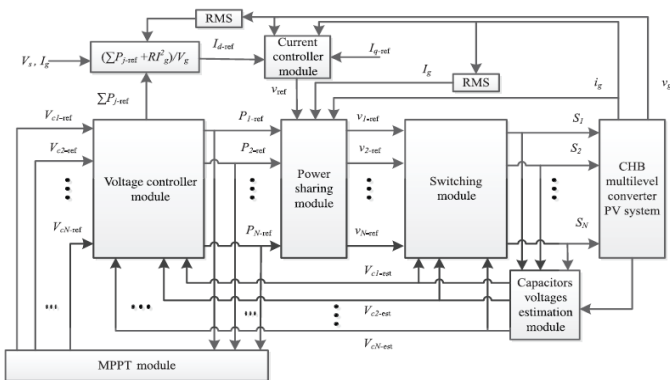


Fig. 2. Block diagram of the dc-side sensor-less CHB-MC-based PV control system

The estimated capacitors' voltages are then used 1) as feedback signals in the voltage controller module; 2) for feedforward compensation of the low-order harmonic ripples in the switching module; and 3) to estimate the average PV modules' power to track the optimal operating point in the MPPT module. The measured grid voltage v_g and the grid current i_g are used by the current controller module. i_g is also used by the power sharing module to generate the voltage reference signals for the switching module.

A. Capacitors' Voltages Estimation Module:

The capacitors' voltages are estimated using a single-voltage sensor that measures the ac output voltage v at the ac-side of the CHB-MC. This allows eliminating all dc-side voltage measurement sensors. The measured ac output voltage v is sampled after each switching transition. Therefore, the voltage sampling frequency for each bridge is twice the switching frequency. The ac output voltage v in an $(N + 1)$ -level CHB-MC is given by

$$v = \sum_{j=1}^N S_j V_{e-j} - DV_{diode} - MV_{switch} \quad (1)$$

where $S_j = (0, +1, -1)$ is the switching function of the j th H-bridge, and V_{diode} and V_{switch} are the forward voltage drops across the conducting diode and switch, respectively. D and M represent the number of conducting diodes and switches, respectively, which can be calculated as [23]

$$D = 2P + Z \quad (2)$$

$$M = 2A + Z \quad (3)$$

In Fig. 3, the voltage sampling instances for a seven-level CHB-MC (three H-bridges) are shown. As it can be observed, the sampling frequency is fixed at twice the switching frequency, which results in high resolution of the estimated capacitors' voltages.

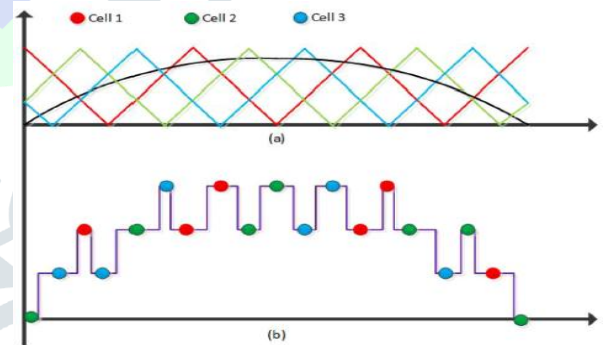


Fig. 3. (a) Reference voltage and carriers. (b) Voltage estimation instances

The generated ac output voltage undergoes transients after each switching transition due to parasitic capacitances and inductances. Therefore, to allow sufficient time for the transients to decay and perform the measurement in the steady state, the measurement is performed after a time delay. However, when the pulse width is too narrow, there is not enough time to perform the estimation.

B. Voltage Controller Module:

The voltage controller module is shown in Fig. 4. The voltage controller module consists of the proportional-integral (PI) voltage controllers, which control each capacitor's voltage toward the reference values determined by the incremental conductance algorithm implemented in the MPPT module.

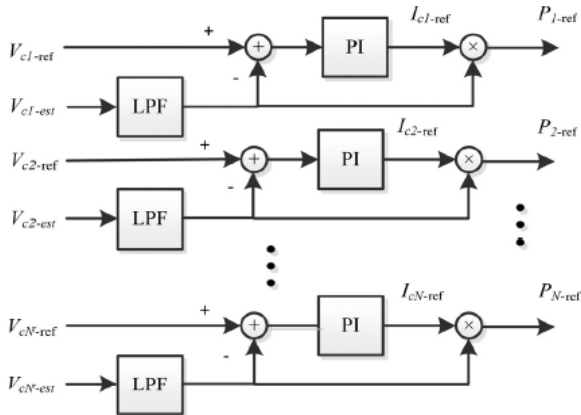


Fig. 4. Voltage controller module

C. Current Controller Module:

Block diagram of the current controller module is shown in Fig. 5. The current controller module controls the grid current in the d-q reference frame. As the system is single phase, the required quadrature signal of the grid current is generated by a quarter of a period delay function.

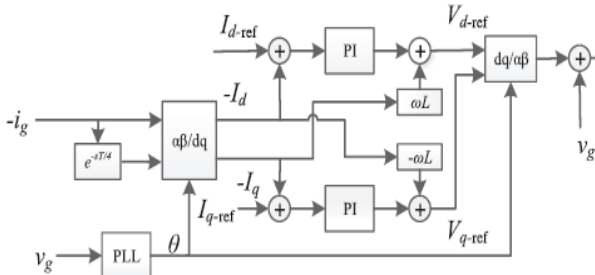


Fig. 5. Current controller module

IV. INCREMENTAL CONDUCTANCE MPPT

In incremental conductance method the array terminal voltage is always adjusted according to the MPP voltage it is based on the incremental and instantaneous conductance of the PV module.

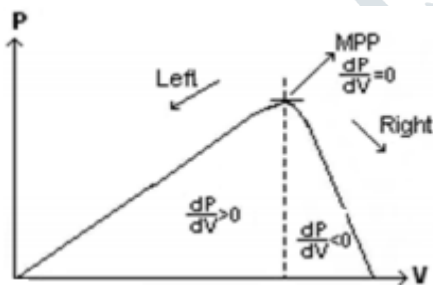


Fig-6: Basic idea of incremental conductance method on a P-V Curve of solar module

Fig-6 shows that the slope of the P-V array power curve is zero at The MPP, increasing on the left of the MPP and decreasing on the Right hand side of the MPP. The basic equations of this method are as follows.

$$\frac{dI}{dV} = -\frac{I}{V} \text{ At MPP} \tag{4}$$

$$\frac{dI}{dV} > -\frac{I}{V} \text{ Left of MPP} \tag{5}$$

$$\frac{dI}{dV} < -\frac{I}{V} \text{ Right of MPP} \tag{6}$$

Where I and V are P-V array output current and voltage respectively. The left hand side of equations represents incremental conductance of P-V module and the right hand side represents the instantaneous conductance. When the ratio of change in output conductance is equal to the negative output conductance, the solar array will operate at the maximum power point.

ALGORITHM:

This method exploits the assumption of the ratio of change in output conductance is equal to the negative output Conductance Instantaneous conductance. We have,

$$P = VI \tag{7}$$

Applying the chain rule for the derivative of products yields to

$$\frac{\partial P}{\partial V} = [\partial(VI)]/\partial V \tag{8}$$

At MPP, as $\partial P/\partial V = 0$ (9)

The above equation could be written in terms of array voltage V and array current I as

$$\frac{\partial I}{\partial V} = -I/V \tag{10}$$

The MPPT regulates the PWM control signal of the dc - to - dc boost converter until the condition: $(\partial I/\partial V) + (I/V) = 0$ is satisfied.

In this method the peak power of the module lies at above 98% of its incremental conductance. The Flow chart of incremental conductance MPPT is shown below.

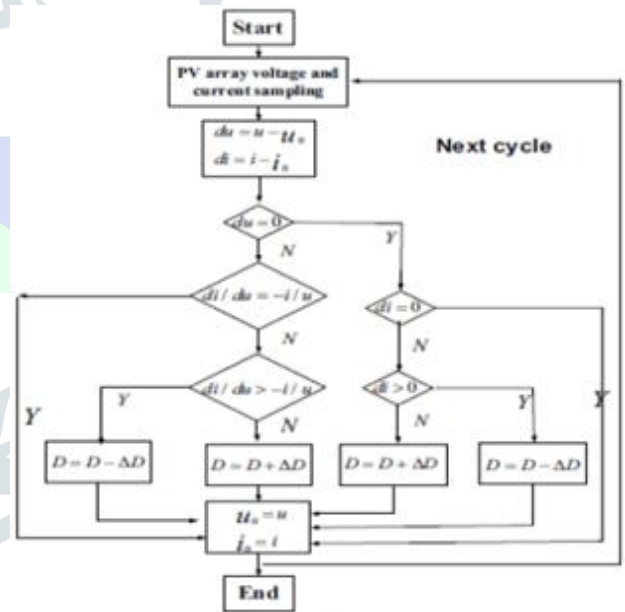


Fig-7: Incremental conductance MPPT Flow chart

VI. SIMULATION RESULTS

A PV array connected to the grid through a nine-level CHB converter is used to simulate the operation of the proposed dc-side sensor-less system. The PV array is composed of four subarrays and each subarray has two series connected REC220AE-US PV modules. Each subarray feeds one H-bridge. The parameters of the simulated system are given in Table I.

TABLE I: PARAMETERS OF THE SIMULATED SYSTEM

Symbol	Quantity	Value
V_{r-gms}	Grid voltage rms value	110 V
C	H-bridge dc capacitance	$3.3 \times 10^{-3} F$
L	Filter inductance	2 mH
f_s	Switching frequency	1600 Hz

f_g	Grid frequency	50 Hz
S	Converter nominal power	1.8 kVAR
R	Filter inductor series resistance	0.2 Ω
f_v	Bandwidth of the voltage controller	10 Hz
f_i	Bandwidth of the current controller	200 Hz
f_m	MPPT update frequency	1 Hz
N	Number of H-bridges	4

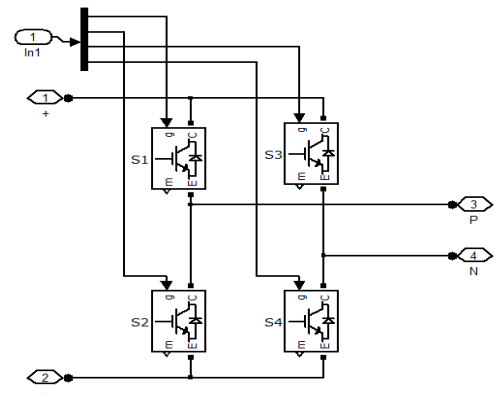


Fig.11. Matlab circuit for cascaded H-bridge circuit

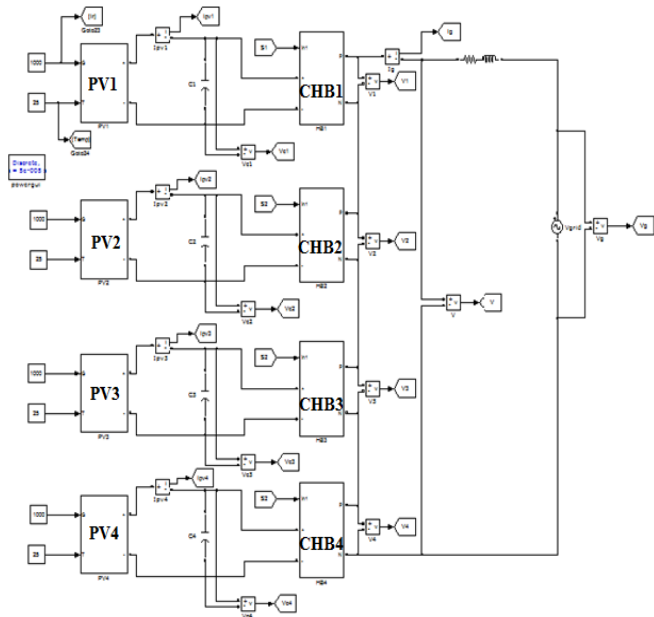


Fig.8. Matlab circuit model for the proposed system

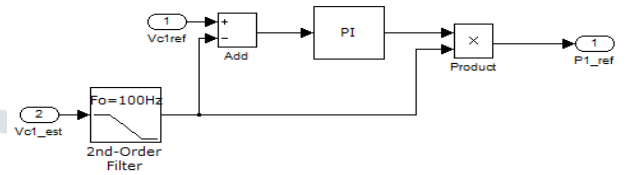


Fig.12. Voltage Controller mode matlab model

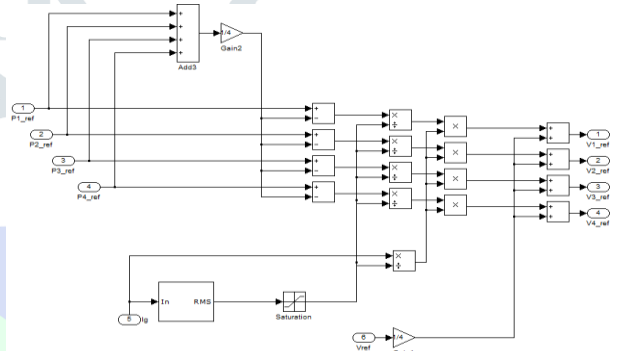


Fig.13. Power Sharing mode matlab model

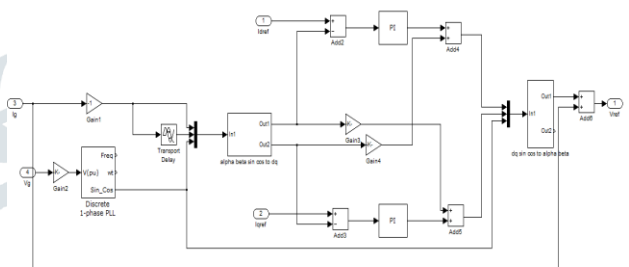


Fig.14. Current Controller mode matlab model

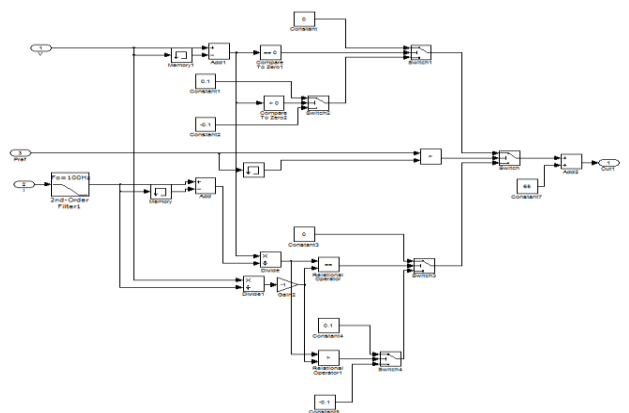


Fig.15. INC based MPPT matlab model

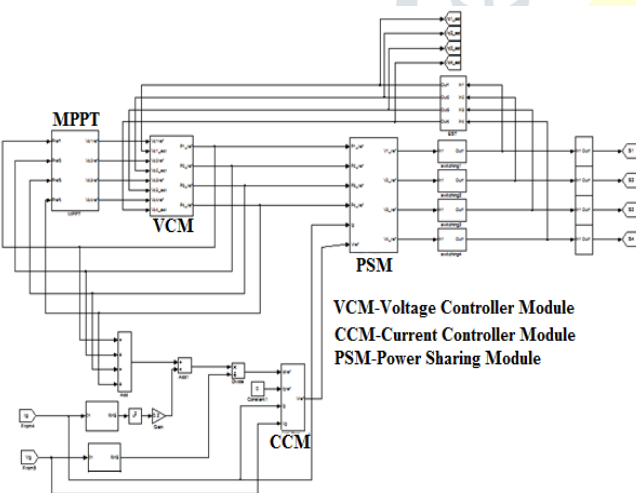


Fig.9. Matlab circuit for CHB-MC based PV control system

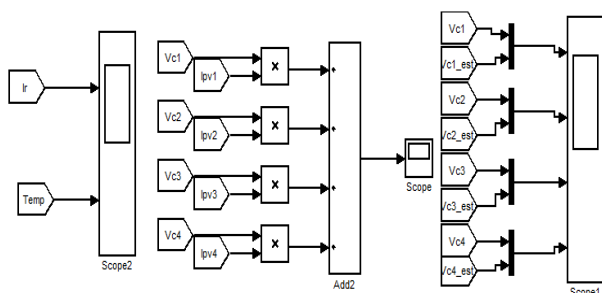


Fig.10. Scopes for output waveforms

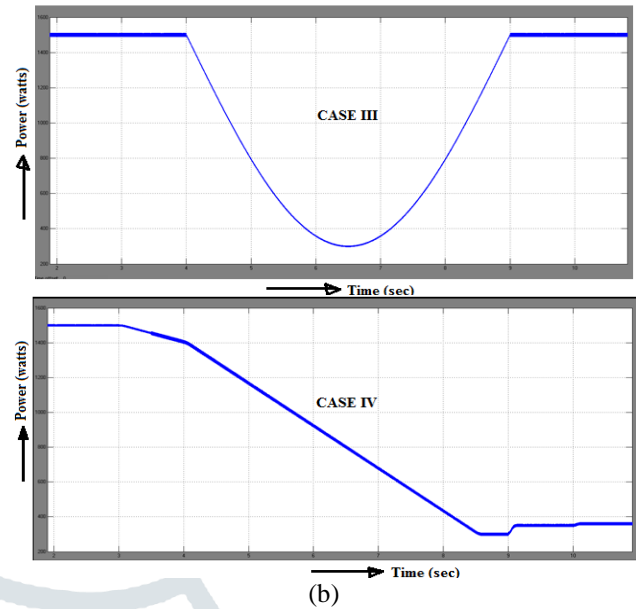
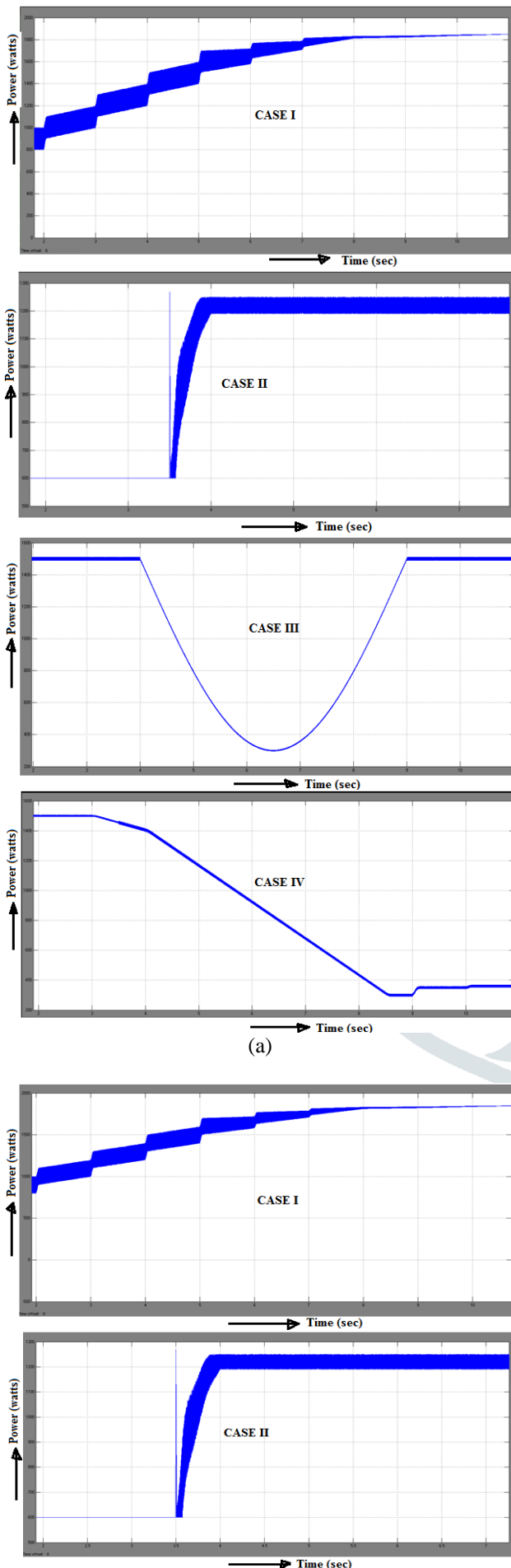


Fig.16. (a) Output power of the proposed PV system. (b) Output power of a conventional system with one dc voltage and one dc current sensor per H-bridge. Case I: startup test. Case II: step irradiance change from 400 to 800W/m² at t = 3.5 s. Case III: gradual irradiance change. Case IV: gradual temperature change.

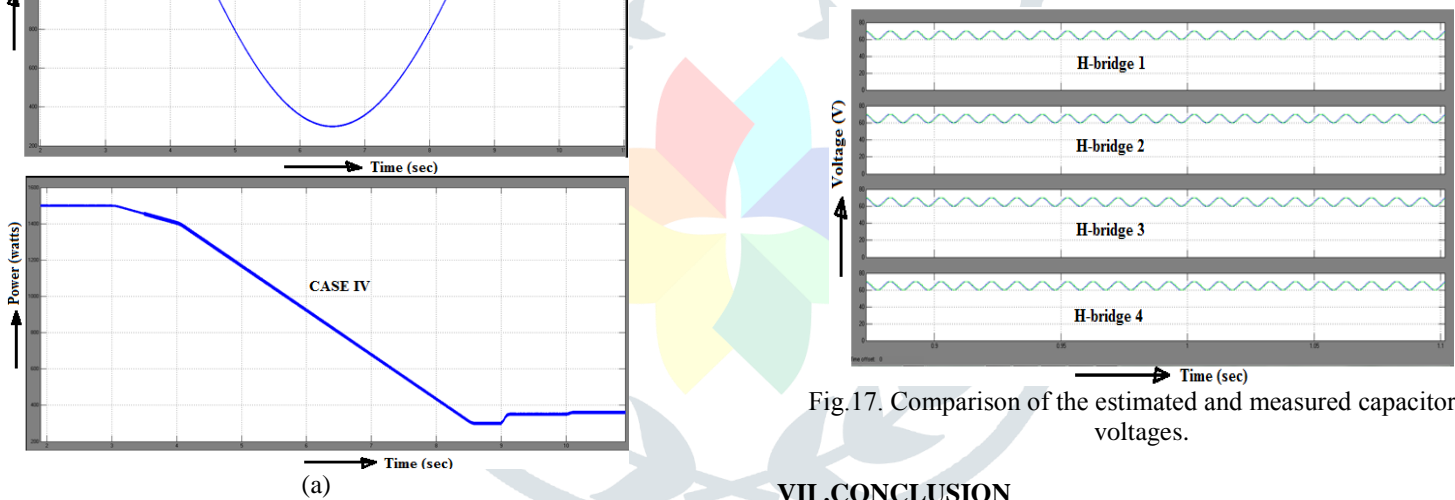


Fig.17. Comparison of the estimated and measured capacitors' voltages.

VII. CONCLUSION

A dc-side sensor-less CHB-MC-based PV system has been proposed and simulated by using MATLAB/Simulink software. In this incremental conductance based MPPT algorithm was used. The simulation tests on a seven-level CHB MC-based PV system showed that the performance of the proposed system was comparable with a conventional system that utilized all dc-side sensors. The main benefits of eliminating the dc-side sensors are reduced price, simpler hardware, and increased reliability of the PV system. The operation of the proposed control system beneath the switching devices failure has not been addressed in this work and needs to be studied in detail in the future to boost the reliability of the system. The simulation was done by using MATLAB/SIMULINK software.

REFERENCES

[1] O. Alonso, P. Sanchis, E. Gubia, and L. Marroyo, "Cascaded H-bridge multilevel converter for grid connected photovoltaic generators with independent maximum power point tracking of each solar array," in Proc. 34th IEEE Power Electron. Spec. Conf. (PESC), 2003, vol. 2, pp. 731-735.

- [2] E. Villanueva, P. Correa, J. Rodriguez, and M. Pacas, "Control of a single-phase cascaded H-bridge multilevel inverter for grid-connected photovoltaic systems," *IEEE Trans. Ind. Electron.*, vol. 56, no. 11, pp. 4399–4406, Nov. 2009.
- [3] S. Kouro, W. Bin, A. Moya, E. Villanueva, P. Correa, and J. Rodriguez, "Control of a cascaded H-bridge multilevel converter for grid connection of photovoltaic systems," in *Proc. 35th Annu. Conf. IEEE Ind. Electron. (IECON)*, 2009, pp. 3976–3982.
- [4] C. Cecati, F. Ciancetta, and P. Siano, "A multilevel inverter for photovoltaic systems with fuzzy logic control," *IEEE Trans. Ind. Electron.*, vol. 57, no. 12, pp. 4115–4125, Dec. 2010.
- [5] J. J. Negroni, D. Biel, F. Guinjoan, and C. Meza, "Energy-balance and sliding mode control strategies of a cascade H-bridge multilevel converter for grid-connected PV systems," in *Proc. IEEE Int. Conf. Ind. Technol. (ICIT)*, 2010, pp. 1155–1160.
- [6] M. Chithra and S. G. B. Dasan, "Analysis of cascaded H bridge multilevel inverters with photovoltaic arrays," in *Proc. Int. Conf. Emerg. Trends Elect. Comput. Technol. (ICETECT)*, 2011, pp. 442–447.
- [7] S. Rivera, S. Kouro, B. Wu, J. I. Leon, J. Rodriguez, and L. G. Franquelo, "Cascaded H-bridge multilevel converter multistring topology for large scale photovoltaic systems," in *Proc. IEEE Int. Symp. Ind. Electron. (ISIE)*, 2011, pp. 1837–1844.
- [8] S. Rivera, W. Bin, S. Kouro, W. Hong, and Z. Donglai, "Cascaded Hbridge multilevel converter topology and three-phase balance control for large scale photovoltaic systems," in *Proc. 3rd IEEE Int. Symp. Power Electron. Distrib. Gener. Syst. (PEDG)*, 2012, pp. 690–697.
- [9] J. Chavarria, D. Biel, F. Guinjoan, C. Meza, and J. J. Negroni, "Energybalance control of PV cascaded multilevel grid-connected inverters under level-shifted and phase-shifted PWMs," *IEEE Trans. Ind. Electron.*, vol. 60, no. 1, pp. 98–111, Jan. 2013.
- [10] F. Wu, B. Sun, J. Duan, and K. Zhao, "On-line variable topology-type photovoltaic grid-connected inverter," *IEEE Trans. Ind. Electron.*, vol. 62, no. 8, pp. 4814–4822, Aug. 2015.